Representations of the occupation number matrix on the LDA/GGA+*U* method

2008 J. Phys.: Condens. Matter 20 325205

(http://iopscience.iop.org/0953-8984/20/32/325205)

IOP PUBLISHING JOURNAL OF PHYSICS: CONDENSED MATTER

J. Phys.: Condens. Matter **20** (2008) 325205 (12pp) doi:10.1088/0953-8984/20/32/325205

Representations of the occupation number matrix on the LDA/GGA + U method

C Tablero

Instituto de Energía Solar, Universidad Politécnica de Madrid, Ciudad Universitaria s/n, E-28040 Madrid, Spain

Received 22 February 2008, in final form 24 June 2008
Published 9 July 2008
Online at stacks.iop.org/JPhysCM/20/325205

Abstract

An analysis of the general representation of the occupation number matrix on density functional theory in conjunction with the generalized Hubbard model is presented. A central fact that will be addressed is that the total charge density cannot be broken down into simple atomic contributions. This fact means that the orbital occupations are not well defined. Different representations of the occupation number matrix, both that it conserves and that it does not conserve the number of electrons of the system, are compared. A localized basis set is used, which is suitable for large-scale electronic structure calculations based on the density functional theory. This methodology is applied to typical and well-analysed transition-metal oxide bulk systems and to Cr-doped zinc chalogenides and chalcopyrites. The bandgap, magnetic moment and detailed electronic structures are investigated and discussed with the different choices of the occupation number matrix. The results are in good agreement with previous theoretical and experimental studies.

(Some figures in this article are in colour only in the electronic version)

1. Introduction

The transition-metal monoxides MnO, FeO, CoO and NiO occupy a special place in condensed-matter physics, because they are regarded as prototypes of the Mott-insulator concept [1]. These materials are antiferromagnetic, electrically insulating, ionic compounds forming in a rocksalt structure. They were among the first highly correlated systems found, where band theory fails to describe a wide range of physical properties. It is mainly the large size of the insulating gap, and often the occurrence of a gap at all, which cannot be explained adequately in one-particle band-structure formalisms [2] such as the local spin density (LDA) and generalized gradient approximation (GGA). A strong Coulomb correlation between the d electrons is responsible for the insulating nature of the monoxides. The d electrons remain localized at the metal ions, because of their Coulomb correlation. It prevents them from forming an incompletely filled d-band. It is this coexistence of local and band-like features in the electronic structure and the resulting physical properties such as the occurrence of the large insulating gaps in the transition-metal monoxides which has led to the longstanding interest in these materials. It has led to the intensification of both theoretical [3–15] and experimental research into the electronic structure of these compounds. No unified theoretical approach is currently available which can describe the electronic properties of the monoxides. In particular, single-particle band-structure calculations cannot reproduce the measured gap widths of the oxides. The reason for these discrepancies is the strong Coulomb interaction between the d electrons in the oxides, which cannot be treated correctly in single-particle band-structure calculations. This Coulomb correlation prevents the electrons from forming d-bands and localizes them at the transition-metal ions. Recent theoretical work [3–15] on the transition-metal oxides introduces more realistic electron interactions and correlations into band-structure calculations and therefore tries to integrate the Mott–Hubbard or charge-transfer picture into band models.

The LDA and GGA approaches for calculating ground-state properties have been widely successful for a wide range of materials [2]. However, in cases where local correlations are strong, they tend to become less accurate or break down. Despite these difficulties, the LDA/GGA has been used successfully to calculate the local Coulomb-interaction parameters in many cases where correlation effects are weak. Some of the failures of the LDA/GGA to describe the ground-state properties of some strongly correlated systems are due to a non-physical interaction of an electron with itself. The LDA/GGA is known to fail particularly badly for transition-metal oxides, giving much too small or zero bandgaps and, in

some cases, too small magnetic moments as well. Therefore, one of the fundamental problems intrinsic to the semilocal functionals is the presence of self-interaction. A direct consequence of the self-interaction in LDA/GGA is that the Kohn–Sham (KS) potential becomes too repulsive and exhibits an incorrect asymptotic behaviour. In general, self-interaction free potentials bind more than LDA/GGA and one expects larger gaps.

Attempts to go beyond LDA/GGA [2] are based on the self-interaction-corrected density functional theory (SIC-DFT), the LDA/GGA+U method, the so-called B3LYP hybrid density functional and the GW approximation. These methods represent corrections of the single-particle KS potential in one way or another and lead to substantial improvements in the LDA/GGA results for the values of the energy gap and local moment. Within the SIC-DFT and LDA/GGA + U methods the self-interaction is subtracted explicitly. It results in a splitting of occupied and unoccupied states by the substantial on-site Coulomb interaction, which is an essential aspect of the physics of Mott insulators. In the B3LYP functional the spurious self-interaction is reduced through the Hartree–Fock exchange, and the hybrid functional treats the correlation more appropriately by optimizing the coefficients of the various terms describing the correlation effects. The GW method goes one step further by calculating the self-energy to the lowest order in the screened Coulomb interaction, and the obtained band structure shows a better agreement. Nevertheless, the GW method, based on the perturbative random-phase approximation, is computationally demanding. The LDA + DMFT approach also combines band-structure theory within the LDA approximation with the many-body theory as provided by dynamical mean-field theory (DMFT). Within DMFT, a lattice model is mapped onto an effective impurity problem embedded in a medium which has to be determined self-consistently, for example, by quantum Monte Carlo simulations. This mapping becomes exact at the limit of infinite dimensions. Therefore, compared with the LDA/GGA, the previous methods capture the physics of transition-metal oxides more correctly and improve the results for the energy gap and local moment significantly.

A large number of studies of transition-metal monoxides have been carried out [3–15], differing in the basis used and/or the details of the approximations. Furthermore, different implementation schemes lead to quite different results regarding the value of the insulating gap and the relative positions of the energy bands. The B3LYP functional has been successfully applied to strongly correlated systems and semiconductors of different bonding types [3] and NiO [4]. Other previous methods have also been applied: the SIC-LDA to transition-metal oxides [5], molecules and solids [6]; the LDA + DFMT to the NiO [7]; the GGA + U to transition-metal oxides for obtaining the oxidation energies [8], the GW method to different systems [9, 10], etc. Also, different implementations of the LDA + U within the all-electron projector augmented-wave method [11], full-potential linearized augmented plane-wave method [12], rotational-invariant form based on a linear response approach [13] and with localized pseudoatomic basis sets [14–17] have been carried out.

Among various approaches, the LDA/GGA + U method [18] is one of the simplest orbital-dependent functionals in which a generalized Hubbard model is introduced in order to treat the localized electrons. It is also one of the least computationally demanding. Because of the simple treatment of the on-site Coulomb correlation effect and the modest computational time, LDA/GGA + U can be considered as one of the most efficient approaches for the description of large-scale correlated systems. However, it should be noted that, although the use of a localized basis set is natural for the implementation of LDA/GGA + U methods, there has been some ambiguity in the definition of the occupation number.

The charge density contains two types of term. With a localized basis set, one term consists of atom-centred contributions (monocentric) and is clearly identified as a contribution to the charge of the atom where the functions are localized. The other contributions, bicentric, correspond to the product of functions located at different atoms. The bicentric contribution cannot be assigned uniquely to any atom. Therefore, the populations are not unique. Moreover, the population scheme depends on the choice of the basis set. If the overlap matrix is the identity, the overlap densities will be zero. The total charge will then be divided formally between the atoms alone. For example, when the overlap matrix is not the identity matrix, the Mulliken decomposition [2], which assigns half of each term to the atoms, is widely used. However, the Mulliken population, like all population analyses, is arbitrary and dependent on the flexibility of the basis set. Other possible choices [2] are: Löwdin population, projections on normalized atomic orbitals, projections on Wannier functions, angular momentum decomposed radial charge around the atoms, etc.

A statement that must be stressed is that the total charge density cannot be broken down into simple atomic contributions. This fact means that the orbital occupations, which are the centrepiece of the LDA/GGA + U approach, are unfortunately not well defined. Therefore, a central fact that will be addressed is the influence of the orbital occupations within the LDA/GGA + U approach.

Using a localized basis set with several representations of the occupation number matrix within the LDA/GGA+U band-structure scheme, the electronic structures of several transition-metal oxides (MnO, FeO, CoO and NiO) have been analysed. Some of the representations of the occupation matrix preserve the original concept of atomic density and the conservation of the electron number of the system, and others do not make it. We compare the physical quantities obtained by introducing these general representations with other definitions suggested before.

In order to analyse the effect of different LDA/GGA + U calculation schemes on other systems, we have chosen some systems with a partially full intermediate band (IB): in particular, the Cr-doped zinc chalogenides ($Cr_xZn_{1-x}S$, with $x = 1/32$) and the Cr-doped chalcopyrite ($Cr_xGa_{1-x}CuS_2$, with $x = 1/16$). The interest in these systems is both technological and theoretical. Technologically, these crystals have very recently attracted the attention of researchers as magnetic semiconductors for spintronics and intermediate-band solar cells. Cr can be incorporated into the wide-bandgap semiconductor, such as ZnS or ZnSe, and exhibits

room-temperature operation in the mid-infrared. Theoretically, because of the narrow and partially filled IB characteristics, the correlation effects should be very important. The IB electrons are supposed to spend their time in regions (around the ions) where the presence of other electrons would make them feel strong Coulomb repulsion, thus correlating their motion. In references [16, 17] the bulk systems $Cr_xZn_{1-x}X$ with X = S and Se and $x \leqslant 0.0625$, with an IB for the majority spin component, are analysed theoretically with the LSDA + U methodology for a wide range of U. The results of the LSDA + U method seem surprising due to the small influence of the U parameter on the electronic properties of the IB. The shift in the position and splitting of the partially filled IB because of the local Coulomb interaction U is very small. The Coulomb interaction induces almost no changes in the occupied bands (the full VB and the partially filled IB). The expected shift in the Cr d-bands is indeed observed in the CB. We analyse this behaviour as a function of the calculation scheme and the occupation matrices.

This paper is organized as follows. In section 2.1 the LDA/GGA + U computational scheme used is presented. The general basis for modelling the occupation number matrix is discussed in section 2.2 and details of the implementation will be set out. The results are discussed and compared with the experiment in section 3, and finally we conclude this paper in section 4

2. Methodology

In this section we derive the fundamental equations for the representation of the occupation number matrix, while looking closely at the main approximations involved in comparison to other representations. Our practical implementation of the LDA/GGA + U method and the occupation matrices are also described.

2.1. LDA/GGA + U total energy functional

The currently used exchange and correlation functionals are built from a homogeneous electron gas so that interactions are treated in a mean-field approach which is not accurate enough to describe correlations properly or account for other many-body effects. Therefore, a further extension beyond the LDA/GGA is carried out using the LDA/GGA + U method [18]. The LDA/GGA + U method is one of the simplest orbital-dependent functionals in which a generalized Hubbard model is introduced in order to treat the localized electrons. The LDA/GGA + U total energy functional is given by adding the energy of a generalized Hubbard model for the localized electrons to the LDA/GGA functional and by subtracting a double counting energy of the localized electrons described in a mean-field sense. The approach used as the starting point corresponds to the fully localized limit: (FLL) LDA/GGA + U,

$$E_{\mathrm{LDA/GGA}+U}[\rho^{(\sigma)}, n^{(\sigma)}] = E_{\mathrm{LDA/GGA}}[\rho^{(\sigma)}] + E_U[n^{(\sigma)}] - E_{\mathrm{DC}}[n^{(\sigma)}] \quad (1)$$

where the Hubbard-like functional (E_U) and double counting term (E_{DC}) are

$$E_U = \tfrac{1}{2}U \sum_{m_1,m_2,\sigma} n^{(\sigma)}_{m_1} n^{(-\sigma)}_{m_2} + \tfrac{1}{2}(U-J) \sum_{m_1 \neq m_2,\sigma} n^{(\sigma)}_{m_1} n^{(\sigma)}_{m_2}, \quad (2)$$

$$E_{\mathrm{DC}} = \frac{U}{2} n(n-1) - \frac{J}{2} \sum_{\sigma} n_\sigma (n_\sigma - 1) \quad (3)$$

and where $n_\sigma = \mathrm{Tr}(n^{(\sigma)}_{m_1 m_2}) = \sum_m n^{(\sigma)}_{mm}$, $n = \sum_\sigma n_\sigma$, $n^{(\sigma)}_m = n^{(\sigma)}_{mm}$ and $n^{(\sigma)}_{m_1 m_2}$ are the elements of the occupation number matrix $\mathbf{n}_\sigma$, which is calculated self-consistently within this approach. Additionally, we assumed the screened Coulomb and exchange parameters U and J independent of the magnetic quantum number m, although they are dependent on the quantum number l. These approximations correspond to neglecting the possible non-spherical character of the effective interactions (the dependence of U and J on the magnetic quantum numbers). As well the results are very insensitive to J when $U - J$ is fixed. Therefore, the U and J terms are grouped together into a single effective parameter, and this effective parameter will be referred to as U in this paper.

Both the occupation numbers as well as the effective Coulomb energy U are crucial in the determination of the correlation effects. The screened U parameter can be estimated theoretically using constrained LDA/GGA calculations by varying the occupation numbers of the d orbitals [19, 20]. However, in many cases the value of U obtained theoretically is different from the optimal value determined empirically as a fitting parameter to experimental results. Therefore, this theoretical value must be considered as an approximate value. As has also been previously mentioned, the U depends additionally on the particular implementation of the LDA/GGA + U.

However, equally or more important is the ambiguity in the definition of the occupation number matrix. It is due to the nature of bonding and it can be illustrated in a very simple way. Let us consider for simplicity a diatomic molecule AB, i.e. a bicentric charge distribution D_{AB}. We want to break down this bicentric distribution into two, one associated to the atom A (D_{A}) and the other one to the atom B (D_{B}): $D_{\mathrm{AB}} = D_{\mathrm{A}} + D_{\mathrm{B}}$. But $D_{\mathrm{AB}} = \alpha D_{\mathrm{AB}} + (1-\alpha) D_{\mathrm{AB}}$, i.e. $D_{\mathrm{A}} = \alpha D_{\mathrm{AB}}$ and $D_{\mathrm{B}} = (1-\alpha) D_{\mathrm{AB}}$, where α is an arbitrary parameter. Note that D_{AB}, D_{A}, D_{B} and α depend on the spatial coordinates. Therefore, the breaking down of a multicentre charge distribution is totally arbitrary. It also causes an arbitrary change in the definition of the occupation numbers' matrix. Of course, any decomposition criteria of the electronic density should preserve the original concept of atomic density.

2.2. Orbital occupations

The occupation numbers are crucial in the determination of the correlation effects from a theoretical and computational point of view. As the total charge density cannot be broken down into simple atomic contributions, the orbital occupations, which are the centrepiece of the LDA/GGA + U approach, unfortunately are not well defined. For a localized basis set, this ambiguity in the definition of the occupation number matrix is due to the

nature of the non-orthogonality of the localized basis orbitals. In this section several different definitions of the occupation number matrix are compared and discussed.

The occupation number matrix $\mathbf{n}_\sigma$ can be evaluated from the density operator or by introducing a projection operator $\hat{P}_m^{(\sigma)}$ as $n_m^{(\sigma)} = \sum_\mu q_\mu^{(\sigma)} \langle \varphi_\mu^{(\sigma)} | \hat{P}_m^{(\sigma)} | \varphi_\mu^{(\sigma)} \rangle$, where $\varphi_\mu^{(\sigma)}$ are the KS eigenvectors for the μ state with spin index σ and $q_\mu^{(\sigma)}$ is their occupation. This index μ includes the band and momentum indices. The m index includes the site, angular momentum and multiplicity of basis function indices. For the case of non-orthogonal basis orbitals, however, different sets of occupation number matrices are expected to emerge from different choices of the projection operators $\hat{P}_m^{(\sigma)}$. The effective non-local potential in terms of the projectors is $\hat{V}^{(\sigma)} = \sum_m U_m^{(\sigma)}(1/2 - n_m^{(\sigma)})\hat{P}_m^{(\sigma)}$ and the orbital energy $\varepsilon_{m[\mathrm{LDA/GGA}+U]}^{(\sigma)} = \partial E/\partial n_m^{(\sigma)} = \varepsilon_{m[\mathrm{LDA/GGA}]}^{(\sigma)} + U_m^{(\sigma)}(1/2 - n_m^{(\sigma)})$.

Two choices have been extensively used in previous implementations of LDA/GGA + U. One version totally ignores the overlaps between the non-orthogonal basis set $|\chi_m\rangle$, the so-called *on-site* representation [21]. The projectors for this case (model $m1$) are $\hat{P}_m^{(\sigma)} = |\bar{\chi}_m\rangle\langle\bar{\chi}_m|$, where the basis set $\bar{\chi}_m$ is the biorthogonal or dual basis of the χ_m: $|\bar{\chi}_m\rangle = \sum_i S_{mi}^{-1}|\chi_m\rangle$ with $\langle\bar{\chi}_i|\chi_j\rangle = \delta_{ij}$.The corresponding occupation number matrix is $\mathbf{n}_\sigma^{(1)} = \mathbf{D}_\sigma$, where $\mathbf{D}_\sigma$ is the density matrix of the system. Another version used in the literature [15–17, 20], the so-called *full* representation, takes care of the overlaps (model $m2$). For this choice the projectors are $\hat{P}_m^{(\sigma)} = |\chi_m\rangle\langle\chi_m|$ and the occupation number matrix is $\mathbf{n}_\sigma^{(2)} = \mathbf{S}\mathbf{D}_\sigma\mathbf{S}$. These two occupation number matrices do not conserve the number of electrons, i.e. the trace of the occupation number matrices is not equal to the total number of electrons, although they have the advantage of being Hermitian matrices.

Another definition of the projector and the corresponding occupation number matrix is the so-called '*dual*' or Mulliken representation [14]. The projectors for this case are: $\hat{P}_m^{(\sigma)} = |\chi_m\rangle\langle\bar{\chi}_m|$. In this formulation, the occupation number matrix $\mathbf{n}_\sigma^{(3)} = \mathbf{S}\mathbf{D}_\sigma$ is treated consistently in the same way as in the Mulliken population analysis. This choice has the advantage of conserving the number of electrons, but the projectors and occupation number matrices are not Hermitians. It is solved by doing the transformation $A \to (A + A^\dagger)/2$ in order to make sure that the resulting effective non-local potential becomes Hermitian.

To be consistent with the use of a non-orthogonal basis set with respect to the conservation of the number of electrons of the system, we introduce a general representation of the occupation number matrix and the corresponding projectors.

The population analysis relates $\mathbf{n}_\sigma$ as a function of the band occupations $q_\mu^{(\sigma)}$. In general this relation is a function of the matrix $\mathbf{C}_\sigma$ that related the μ-band with the i-orbital basis set ($|\varphi_\mu^{(\sigma)}\rangle = \sum_i C_{i\mu}^{(\sigma)}|\chi_i\rangle$), the overlapping matrix $\mathbf{S}(S_{ij} = \langle\chi_i|\chi_j\rangle)$ and the density matrix $\mathbf{D}_\sigma = \mathbf{C}_\sigma\mathbf{Q}_\sigma\mathbf{C}_\sigma^\dagger$. The $\mathbf{Q}_\sigma$ is a diagonal square matrix whose elements are the band occupation numbers: $Q_{\mu\nu}^{(\sigma)} = q_\mu^{(\sigma)}\delta_{\mu\nu}$. Both $\mathbf{C}_\sigma$ and $\mathbf{Q}_\sigma$ are obtained in the calculations. The principal population analysis use the property $N_\sigma = \mathrm{Tr}\, z[\mathbf{Q}_\sigma] = \sum_\mu q_\mu^{(\sigma)}$, where $N = \sum_\sigma N_\sigma$ is the total number of electrons. The $\mathbf{Q}_\sigma$ is related to the matrix $\mathbf{n}_\sigma$, in general non-diagonal, so that $N_\sigma = \mathrm{Tr}\, z[\mathbf{n}_\sigma]$. The arbitrariness in the population's analysis is a consequence that: (i) for obtaining the trace of a product of matrices the order of the product of the matrices is not relevant, (ii) the matrix trace is invariant with respect to the similarity transformation: $N_\sigma = \mathrm{Tr}\, z[\mathbf{n}_\sigma] = \mathrm{Tr}\, z[\mathbf{G}_\sigma\mathbf{Q}_\sigma\mathbf{G}_\sigma^{-1}]$, where $\mathbf{G}_\sigma$ is an arbitrary matrix. For example, in the Mulliken population analysis $\mathbf{G}_\sigma^{(M)} = \mathbf{C}_\sigma$, whereas in the Löwdin population analysis $\mathbf{G}_\sigma^{(L)} = \mathbf{S}^{1/2}\mathbf{C}_\sigma$ (unitary matrix). Keeping all of this in mind we can define the projectors $\hat{P}_m^{(\sigma)} = |a_m^{(\sigma)}\rangle\langle b_m^{(\sigma)}|$, where $a_i^{(\sigma)} = \sum_j A_{ij}^{(\sigma)}\chi_j$ and $b_i^{(\sigma)} = \sum_j B_{ij}^{(\sigma)}\chi_j$, with $\mathbf{B}_\sigma = (\mathbf{G}_\sigma\mathbf{C}_\sigma^\dagger)^*$ and $\mathbf{A}_\sigma = (\mathbf{C}_\sigma\mathbf{G}_\sigma^{-1})^T$. With this choice the corresponding representations of the occupation number matrix and the matrix of the non-local LDA/GGA + U potential are $\mathbf{n}_\sigma = (\mathbf{G}_\sigma\mathbf{C}_\sigma^{-1})\mathbf{D}_\sigma(\mathbf{G}_\sigma\mathbf{C}_\sigma^\dagger)^{-1}$ and $\mathbf{V}_\sigma^{(\mathrm{DFT}+U)} = (\mathbf{G}_\sigma\mathbf{C}_\sigma^\dagger)^{-1}\mathbf{V}_\sigma(\mathbf{G}_\sigma\mathbf{C}_\sigma^{-1})$ with $V_{ij}^{(\sigma)} = U_m^{(\sigma)}(1/2 - n_m^{(\sigma)})\delta_{im}\delta_{ij}$. This choice conserves the number of electrons, but the projectors and occupation number matrices are not Hermitians. It is solved by doing the transformation $\mathbf{n}_\sigma \to (\mathbf{n}_\sigma + \mathbf{n}_\sigma^\dagger)/2$ and similarly for $\mathbf{V}_\sigma^{(\mathrm{DFT}+U)}$. In these definitions it is not the overlap matrix explicitly. In order to reflect this fact explicitly and to relate the general matrix $\mathbf{G}_\sigma$ directly with Mulliken and Löwdin population's analyses we will use $\mathbf{G}_\sigma = \mathbf{B}_\sigma\mathbf{S}^\alpha\mathbf{C}_\sigma$, where $\mathbf{B}_\sigma$ is an arbitrary matrix and α is an arbitrary parameter. This way, $\alpha = 0$ or 1 corresponds to the Mulliken population's analyses, and $\alpha = 1/2$ corresponds with the Löwdin population's analyses.

2.3. Implementation details

We will use $\mathbf{G}_\sigma = \mathbf{B}_\sigma\mathbf{S}^\alpha\mathbf{C}_\sigma$ with $\mathbf{B}_\sigma$ equal to the identity matrix for the occupation number matrix and the projectors. These schemes that conserve the number of electrons will be labels like $p(\alpha)$. Note that $p(0)$ corresponds to the Mulliken scheme and $p(1/2)$ to the Löwdin scheme. In general, the calculation of the $\mathbf{S}^\alpha$ is proportional to N^3, where N is the $\mathbf{S}$ dimension. Therefore, this process is computationally expensive. Nevertheless, the computational cost is reduced by doing the approximation to first order: $\mathbf{S}^{-\alpha} \approx \mathbf{I} + \alpha\mathbf{X} = (1 - \alpha)\mathbf{I} + \alpha\mathbf{S}$. The inconvenience of this approximation is that the scheme no longer preserves the total electron number. These schemes that do not conserve the number of electrons will be labelled as $p'(\alpha)$. Neither the schemes $m1$ nor $m2$ conserve the number of electrons. Note that, with the approximation of the $\mathbf{S}^\alpha$ matrix, the $p'(\alpha)$ scheme is a linear combination of the $m1, m2$ and Mulliken schemes: $p'(\alpha) = \alpha(1-\alpha)[m1+m2] + [\alpha^2 + (1-\alpha)^2]p(0)$. In particular $p'(0) = p(0)$ corresponds with the Mulliken scheme.

Note that during the LDA/GGA + U calculations we will use the same scheme for the projectors and for the occupation numbers. We will refer to them as calculation schemes $p(\alpha)$-, $p'(\alpha)$-, $m1$- or $m2$-LDA/GGA + U. However, after the calculation, we can carry out a different population analysis based on the different occupation numbers. Therefore, independently of the LDA/GGA + U calculation scheme, we will also carry out population analysis based on the occupation numbers $p(\alpha)$, $p'(\alpha)$, $m1$ or $m2$.

Table 1. Comparison of the experimental and theoretical magnetic moments of the transition-metal Mott oxides obtained using different schemes. For the LDA/GGA + U schemes the U (eV) value is indicated within parentheses.

$\mu(\mu_B)$	NiO	MnO	FeO	CoO
Expt[a]	1.64–1.90	4.58–4.79	3.32	3.35–3.8
LDA-SIC[b]	1.49	4.64	3.55	2.59
GGA + U [c]	1.72(6.4)	4.65(4)	3.69(4)	2.65(3.3)
LDA + U	1.62–1.79[d] (6), 1.5[e] (6)			
Others	1.56[f] (GW), 1.67[g] (B3LYP)			
This work	1.22–1.90(6)	3.78–5.4(6)	3.1–4.1(4.3)	2.2–3.0(6)

[a] Reference [30]; [b] Reference [5]; [c] Reference [8]; [d] Reference [14]; [e] Reference [31]; [f] Reference [9, 10]; [g] Reference [4].

2.4. Calculations

The electronic structure calculations were carried out by using the DFT [22] method based on pseudopotentials for core electrons and numerically localized pseudoatomic orbitals as the basis set for the valence wavefunctions. The standard KS [23] equations are solved self-consistently [24]. For the exchange and correlation term, the LDA has been used as proposed by Ceperley–Alder [25] and the GGA corrections in the form of Perdew, Burke and Ernzerhof [26]. The standard Troullier–Martins [27] pseudopotential is adopted and expressed in the Kleinman–Bylander [28] factorization. The KS orbitals are represented using a linear combination of confined pseudoatomic orbitals [29]. An analysis of the basis set convergence has also been carried out using from single-zeta to double-zeta with polarization basis sets for all atoms and varying the number of special k points in the irreducible Brillouin zone (BZ). In all calculations a double-zeta with polarization function basis set (DZP) has been used, and we use periodic boundary conditions with 686 special k points in the irreducible BZ.

3. Results

We have used this *ab initio* band-structure scheme to study the electronic structure of MnO, FeO, CoO and NiO. The transition-metal monoxides form ionic, antiferromagnetic crystals with the NaCl structure. The antiferromagnetic order of the transition-metal monoxides MnO, FeO, CoO and NiO is of that type which is often called type II antiferromagnetism. The (111) planes of the transition-metal sublattice are planes of parallel spins; adjacent (111) planes show an antiparallel alignment of the spins. From a simple band-structure point of view, NiO, CoO and MnO should be metals like the corresponding transition metals, as a result of their incompletely filled d states. But, as mentioned previously, they are insulators with wide insulating gaps. Whereas the O states form bands with a dispersion consistent with LDA/GGA band-structure calculations, the application of these calculations to the d metal states produces results in contradiction to a lot of experimental evidence.

3.1. General comparison with other results

Because the majority of calculations in the transition-metal monoxides have been carried out with the experimental lattice spacing, we have also used this experimental lattice constant in order to compare our results with many others in the literature. Although the U values can be obtained theoretically using constrained calculations, we have preferred to use values within the range of those used in the literature. These U values are not the optimal ones. However, these values permit the influence of the different occupation matrices to be shown, which is the aim of this work.

Just like the previous LDA/GGA + U and LDA-SIC calculation results, the typical increase in the bandgaps is observed. The magnitudes of the gaps and the magnetic moments are well compared in a reasonable agreement with experimental results as well as the previous calculations. Tables 1 and 2 illustrate the enhancement of the gaps and magnetic moments. As expected, larger magnetic moments are obtained with LDA/GGA + U, and the values are in good agreement with experiments and previous calculations. The difference between the gaps and magnetic moments from different occupation matrices will be discussed later.

Depending on the U values, there is a substantial combination of the oxygen states with the metal states. The details of this mixture determine the position of the oxygen bands with respect to the metal bands and hence the energy bandgap. These results differ dramatically from those corresponding LDA/GGA results where the top of the valence bands and the bottom of the conduction bands are the metal d states. Therefore, the bandgaps occur in the LDA/GGA, if at all, between metal d states, at variance with experimental evidence. The use of the LDA/GGA + U method for studying FeO and CoO is mainly motivated by the attempt to reproduce the observed insulating behaviour. In fact, standard DFT methods, such as LDA or GGA, produce a non-physical metallic character because neither the crystal field nor electronic structure effects are sufficient in this case to open up a gap. However, using LDA/GGA + U, a gap opens up at around the Fermi level.

In general, with all occupation schemes the GGA + U produces an increase in the gaps and magnetic moments with respect to those of the LDA + U. However, qualitatively, the results are similar.

In general, for the different calculation schemes there is a decrease in both the gap and the magnetic moments with the α increase from 0 to 1/2 for both schemes, $p(\alpha)$ and $p'(\alpha)$: $p(1/2) \leqslant p(\alpha) \leqslant p(0)$-LDA/GGA + U and $p'(1/2) \leqslant p'(\alpha) \leqslant p'(0)$-LDA/GGA+$U$. For α fixed, there is a decrease in both the magnetic moments and the gaps as the calculation

Table 2. Comparison of the experimental and theoretical gaps in the transition-metal Mott oxides obtained with different schemes. For the LDA/GGA + U schemes the U (eV) value is shown in brackets.

Gaps (eV)	NiO	MnO	FeO	CoO
Expt	4.0–4.3[a]	3.6–3.8[b]	2.4[c]	2.4[d]
LDA-SIC[e]	2.66	3.57	3.25	2.51
GGA + U [f]	3.4(4)	3.2(4)	2.2(4)	2.0(3.3)
LDA + U	3.89[g] (6), 3.1[h] (7.05), 2.7[i] (6)	4.21[g] (6), 3.5[h] (6.04)	2.77[g] (6), 3.2[h] (5.91), 2.0[j] (4.3)	3.01[g] (6), 3.2[h] (6.88)
Others	3.7[k] (GW), 4.2[l] (B3LYP)			
This work	2.8–3.9(6)	1.8–2.6 (6)	1.9–2.7(4.3)	1.21–2.72(6)

[a] Reference [32]; [b] Reference [33]; [c] Reference [34]; [d] Reference [35]; [e] Reference [5]; [f] Reference [8]; [g] Reference [14]; [h] Reference [20]; [i] Reference [31]; [j] Reference [13]; [k] Reference [9, 10]; [l] Reference [4].

schemes change from $p(\alpha) \geqslant p'(\alpha) > m2$-LDA/GGA + U and $p'(\alpha) \geqslant p(\alpha) > m2$-LDA/GGA + U, respectively. Note that, with α very small, $p'(\alpha) \approx p(\alpha)$. The behaviour of the magnetic moments is independent of the occupation number matrices used, after the calculation, to obtain the magnetic moments.

From a numerical point of view, the robustness of the convergence in the self-consistency iterations depends on the definition of the occupation number matrix discussed in section 2. Because the calculation of the $\mathbf{S}^{\alpha}$ in each cycle is proportional to N^3, where N is the $\mathbf{S}$ dimension, the LDA/GGA + U calculations based on the $p(\alpha)$ scheme is slower than that based on $p'(\alpha)$. The convergence of the $p(\alpha)$ scheme is similar for $0 \leqslant \alpha \leqslant 1/2$, except for α next to zero. For the $p'(\alpha)$ scheme, the convergence rate for α next to zero is also slower. In this case the $p'(\alpha)$ scheme is similar to the $p(\alpha)$ scheme.

With multiple-zeta and polarization orbitals it is not clear how the LDA/GGA + U calculation will be affected by the use of these types of basis set. In particular when we apply the self-interaction correction to the transition-metal d orbitals for a DZP basis set with two d-shells, we have several options: to apply a self-interaction U_1 to the first shell and zero for the second shell, zero for the first shell and U_2 for the second shell, and U_1 to the first shell and U_2 for the second shell. The result demonstrates that the calculated electronic structure is not greatly affected by the use of additional multiple-zeta orbitals whenever the self-interaction is included for the more confined d-shell. To include the self-interaction within more d-shells increases the gap slightly. However, to not include the first d-shell brings about a great reduction in the gap with results more similar to LDA/GGA. Thus, we use the basis set subspace consisting of the more confined d-shell for the self-interaction correction.

3.2. NiO

LDA/GGA produced an antiferromagnetic insulating ground state with a small bandgap and a small magnetic moment with respect to the experimental values (tables 1 and 2). The most interesting feature of our LDA/GGA is that the d states of Ni dominate the region in the vicinity of the bandgap: the top of the valence band has a t–d Ni character and the bottom of the conduction band is made up of the e–d Ni orbitals.

With LDA/GGA + U we have applied the self-interaction correction only to the occupied transition-metal 3d states using an intermediate U of 6 eV in accordance with results reported in the literature. In agreement with previous LDA/GGA + U calculations, the spin majority e_+ states are pushed towards lower energies. The Ni e_+ peak occurs about 7–8 eV below the valence-band edge, which is in good agreement with the position of the experimentally observed [32–36] and of the theoretically calculated [4, 5, 7, 10–14]. Consequently, the Ni 3d bands are closer to the region where the O orbitals contribute more, because of the Hubbard interaction. These results differ dramatically from the corresponding LDA/GGA results where the top of the valence bands and the bottom of the conduction bands are the metal d states. A substantial d-band splitting also occurs because of the self-interaction. The energy difference between e_+ and e_- is about 10 eV for $U = 6$ eV and 13–14 eV for $U = 10$ eV. Here again the GW model yields a value of about 9 eV for this splitting [10], in good agreement with our results for $U = 6$ eV. Nevertheless, different implementations of the GW scheme lead to different results with respect to the gap and the relative positions of the energy bands [9, 10].

In order to gain more insight into the nature of the bandgap in figure 1 we show the total densities of states and their decomposition into the metal and oxygen components for NiO with several schemes of the occupation matrix with LDA + U. Quantitatively the GGA + U produces an increase in the gaps with respect to that of the LDA+U, but qualitatively the results are similar.

The change of the gap with α for the $p(\alpha)$- and $p'(\alpha)$-LDA/GGA + U schemes is shown in figure 2. From this figure we have obtained several conclusions: (i) the gap using GGA+U is larger than when LDA+U is used. This difference is larger for $\alpha = 0$; (ii) for both schemes, $p(\alpha)$ and $p'(\alpha)$, the gaps decrease from $\alpha > 0.13$ to $\alpha = 1/2$, except to the $p'(\alpha)$-LDA+U scheme; (iii) in general, for α fixed and $\alpha > 0.13$, the gap is larger for the $p'(\alpha)$-LDA/GGA + U scheme that for the $p(\alpha)$-LDA/GGA+U scheme; (iv) with the $m2$-LDA/GGA+U scheme, the gaps are lower than that obtained with the $p(\alpha)$ and $p'(\alpha)$ schemes for $0 \leqslant \alpha \leqslant 1/2$.

The change in the magnetic moments with α for the $p(\alpha)$- and $p'(\alpha)$-LDA/GGA + U schemes is shown in figure 3 as a function of α. Note that in the self-consistency iterations we use the same scheme for the occupation matrices and projectors. However, after the calculation, we can use any one of the occupation schemes in order to obtain the magnetic moments. For this reason, although we have used the $p(\alpha)$- and $p'(\alpha)$-LDA/GGA + U schemes for the calculations of this

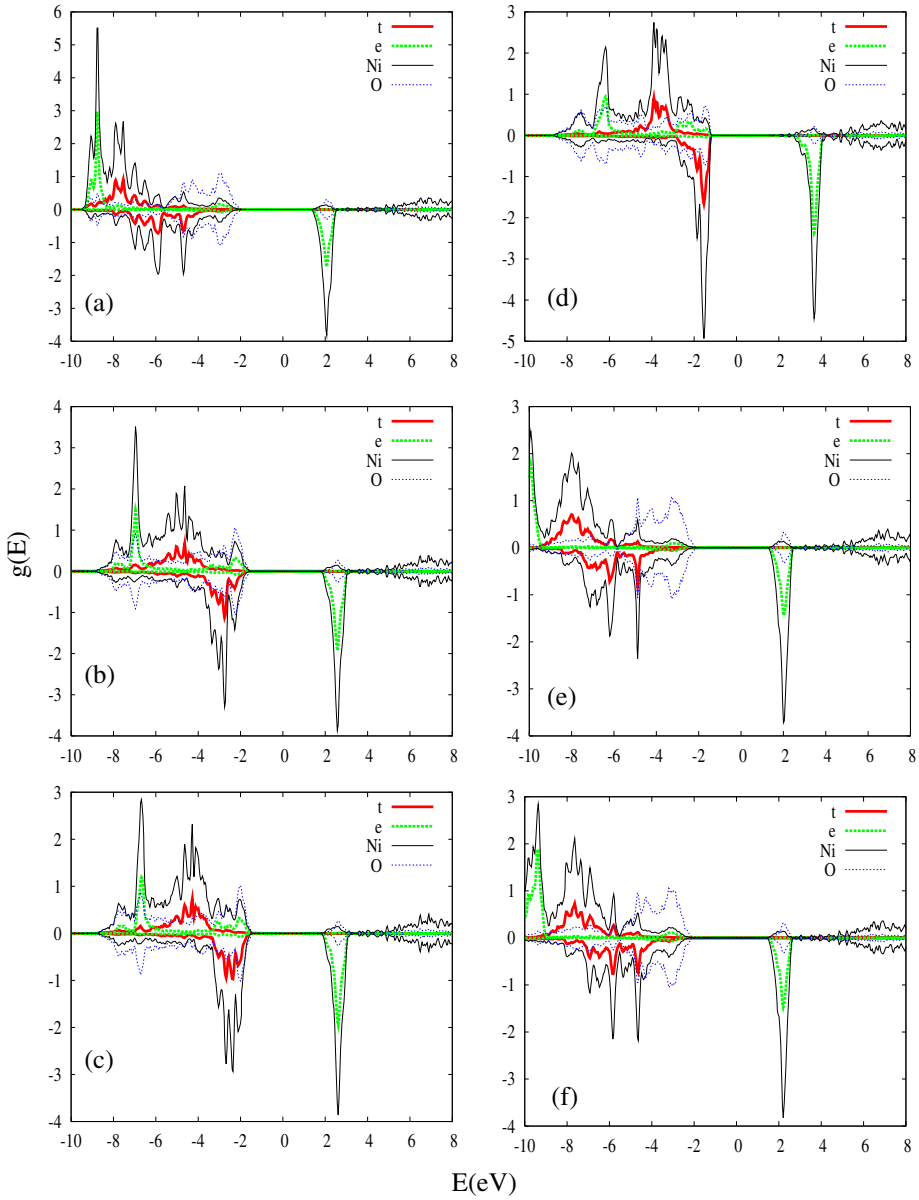

Figure 1. Projected DOS for the NiO on the O and the Ni atoms, as well as the t-Ni and e-Ni orbitals: (a) $p(0.1)$-, (b) $p(0.3)$-, (c) $p(0.5)$-, (d) $m2$-, (e) $p'(0.3)$- and (f) $p'(0.5)$-LDA $+ U$. The Fermi energy as zero has been chosen in this figure.

figure, the magnetic moments have been obtained using the same occupation matrices or others different from those used for the self-consistency calculation. In the figure, the magnetic moments obtained with the $p(\alpha)$ occupation matrices, the same as for the $p(\alpha)$-LDA/GGA $+ U$ calculation, are between the $p(0)$ (Mulliken) and $p(1/2)$ (Löwdin) analyses. When α is very small for the $p'(\alpha)$ analyses, the results (not shown in the figure) are similar to the Mulliken analyses. However, for $1/4 \leqslant \alpha \leqslant 1/2$, the magnetic moment obtained with the $p'(\alpha)$-LDA/GGA $+ U$ scheme decrease with the α increment, and are lower than those calculated with the Mulliken, Löwdin, and in general, with the $p(\alpha)$ scheme. It is interesting to highlight that the magnetic moments, independent of the occupation matrix scheme used to calculate them, are almost constant in the range $0.2 \leqslant \alpha \leqslant 0.5$. Comparing the $p(\alpha)$- and $p'(\alpha)$-LDA/GGA $+ U$ schemes, there are differences until $\pm 1\ \mu_B$ when the same type of occupation matrices are used in order to obtain the magnetic moments.

3.3. MnO

Similar to NiO, the MnO is characterized by partially filled 3d orbitals and an associated local magnetic structure where the Mn atoms are antiferromagnetically aligned. The top of the VB is expected to be of a mixed Mn 3d–O 2p character and the bottom of the CB pure Mn 3d in character. However, the LDA/GGA description of MnO is a narrow gap insulator where the edges of the VB and CB are made up of purely Mn 3d states.

In this case, LDA/GGA $+ U$ also represents a considerable improvement with respect to LDA/GGA. The size of the fundamental gap is more similar to the experimental one and

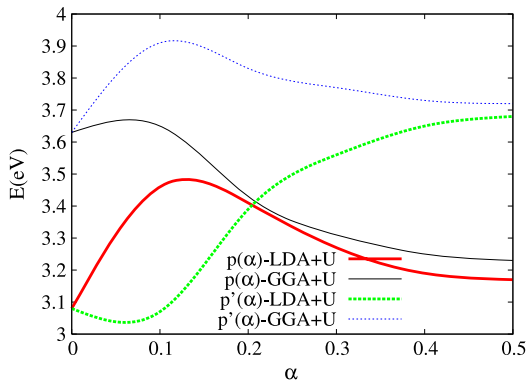

Figure 2. The gap for the NiO as a function of the α parameter for the calculation schemes $p(\alpha)$-GGA $+ U$, $p(\alpha)$-LDA $+ U$, $p'(\alpha)$-GGA $+ U$ and $p'(\alpha)$-LDA $+ U$.

there is an increase in the contribution of the O atom and a decrease in the d-Mn character at the top of the VB with respect to LDA/GGA. However, the contributions from the atoms to the top of the VB depend on the occupation matrices and projectors used in the LDA/GGA $+ U$ scheme.

The magnetic moment calculated using different calculation schemes and occupation matrices are shown in panels (a) of figure 4 for the MnO, and for FeO and CoO in panels (b) and (c), respectively. The behaviour of the magnetic moment of these oxides is similar to the previously analysed NiO. The results are in good agreement with those of the literature [5, 6].

3.4. CoO and FeO

Contrary to the previous cases of NiO and MnO, the LDA/GGA produces an unphysical metallic character in contradiction with observation. For FeO and CoO, the application of the LDA/GGA $+ U$ splits the metallic d-band, within the CB, obtained with the LDA/GGA. This splitting depends on the scheme used by the occupation matrices and projectors during the self-consistency calculation.

The calculated LDA/GGA $+ U$ DOS is shown in figure 5, and it is in agreement with that published in the literature [5, 13, 14], although different implementation schemes lead to different results regarding the gap value (see table 1), magnetic moments (see table 2) and position of the energy bands. Similar to previous transition-metal monoxides analysed, the value of these magnitudes depend on the occupation matrix and projector scheme used for the LDA/GGA $+ U$ calculation. With all schemes used, the partially full metallic d-band in the CB is split into two bands in agreement with that published in the literature. One is empty within the CB, and another one full below the CB. Depending on the scheme, and for $U = 4.3$ eV fixed, the full d-band is within the gap, on top of the VB or within the VB. Of course, an increase in the U value can introduce the full band towards the interior of the VB. Nevertheless, with this U value the results are in reasonable agreement with others published in the literature and with experimental results (see table 1). For the Mulliken and $p'(1/2)$ schemes the splitting of the original LDA/GGA metallic band is larger than for the Löwdin and $m2$ schemes. It also influences the composition of the VB.

For the CoO, the transition-metal sub-band partially filled in the CB for LDA/GGA has one additional electron with respect to the FeO. Therefore, the two bands resulting from the splitting of the partially full metallic d-band when LDA/GGA $+ U$ is applied have different characteristics than for the FeO. For CoO, the empty band within of the CB has a

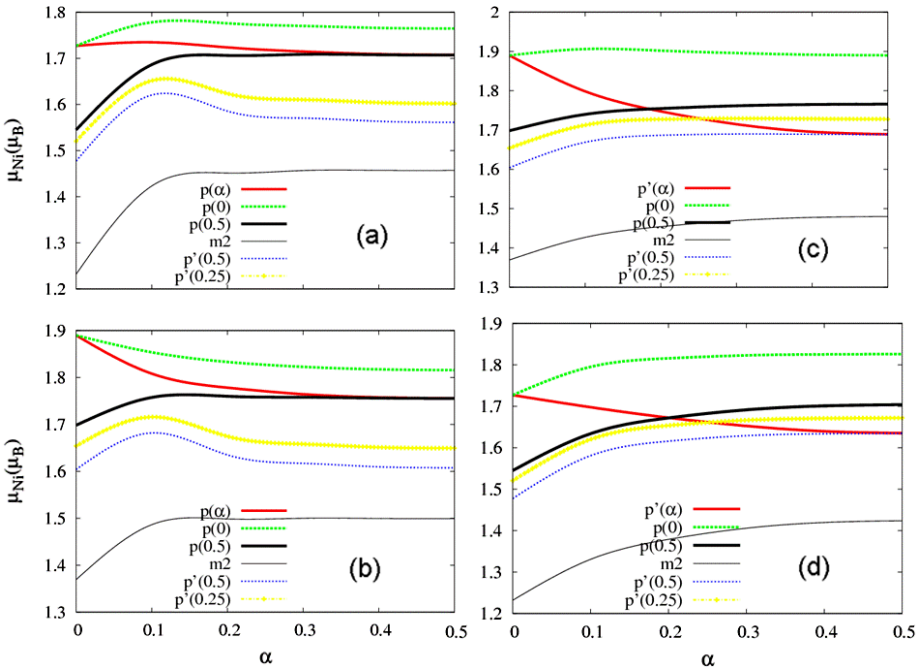

Figure 3. The Ni magnetic momentum (μ_B) for the NiO as a function of the α parameter for the calculation schemes (x axis): (a) $p(\alpha)$-GGA $+ U$, (b) $p(\alpha)$-LDA $+ U$, (c) $p'(\alpha)$-GGA $+ U$, (d) $p'(\alpha)$-LDA $+ U$. The curves $p(\alpha)$, $p(0)$, $p(0.5)$, $m2$, $p'(0.5)$ and $p'(0.25)$ correspond to the different population analyses (occupation number matrices) used to obtain the magnetic momentum.

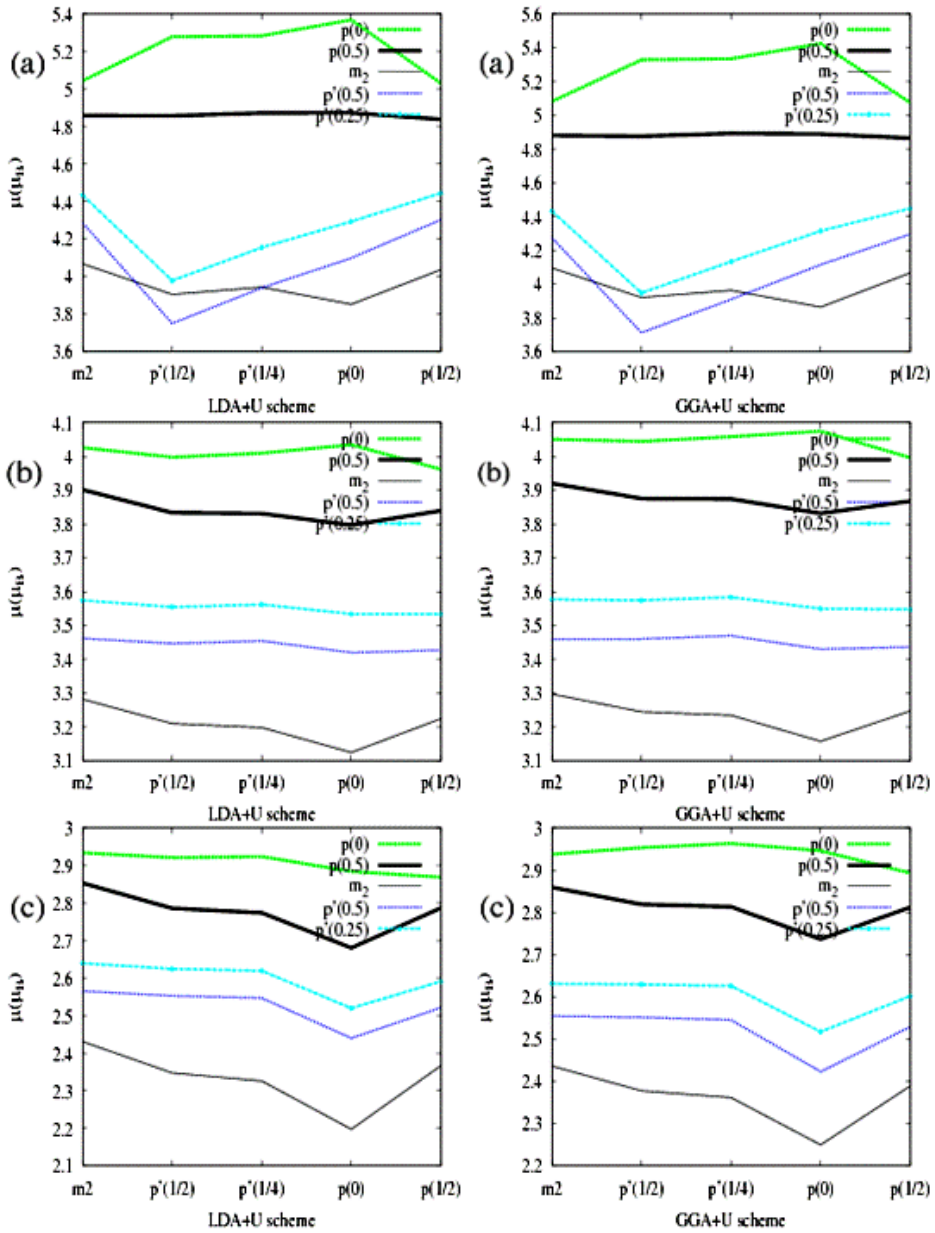

Figure 4. Magnetic momentum (μ_B) of the Mn (a), Fe (b) and Co (c) using different calculation schemes (x axis) $m2$-, $p'(1/2)$-, $p'(1/4)$-, $p(0)$, and $p(1/2)$-LDA + U (left panels) and -GGA + U (right panels), The curves $p(0)$, $m2$, $p'(1/2)$, $p'(1/4)$ and $p(1/2)$ correspond to the different population analyses (occupation number matrices) used to obtain the magnetic momentum.

lower number of states than for the FeO, whereas the full band has a larger number of states than for the FeO.

3.5. Other materials

As was previously mentioned in the introduction, in references [16, 17] the bulk systems $Cr_xZn_{1-x}X$ with X = S and Se and $x \leqslant 0.0625$ were analysed theoretically with the LSDA + U methodology for a wide range of U (from $U = 0$ to 6 eV). In these works, the methodology used was the $m2$-LDA + U for the self-consistent calculation and the $p(0)$-Mulliken occupation matrix for the population analyses. From the results of these works, the systems are characterized by a partially full intermediate band (IB) for the majority spin component. Because of the results in the Mott oxides as a function of the occupation number matrix, in this work we have expanded the study of these systems with different calculation schemes.

3.5.1. Cr-doped zinc chalogenides. In figure 6 we show the projected DOS per atom on Cr, Zn and S atoms for the Cr-doped zinc chalogenides ($Cr_xZn_{1-x}S$, with $x = 1/32$) with $U = 3$ eV using two different LDA + U calculation schemes: $p(1/2)$-LDA + U (panel a) and $p(0)$-LDA + U (panel b). The S atoms can be broken down into two groups: those directly bonded to the Cr atoms and those which are not. Only the contribution of the S directly bonded to the Cr atoms is represented in figure 6. These S atoms, and the Cr atoms,

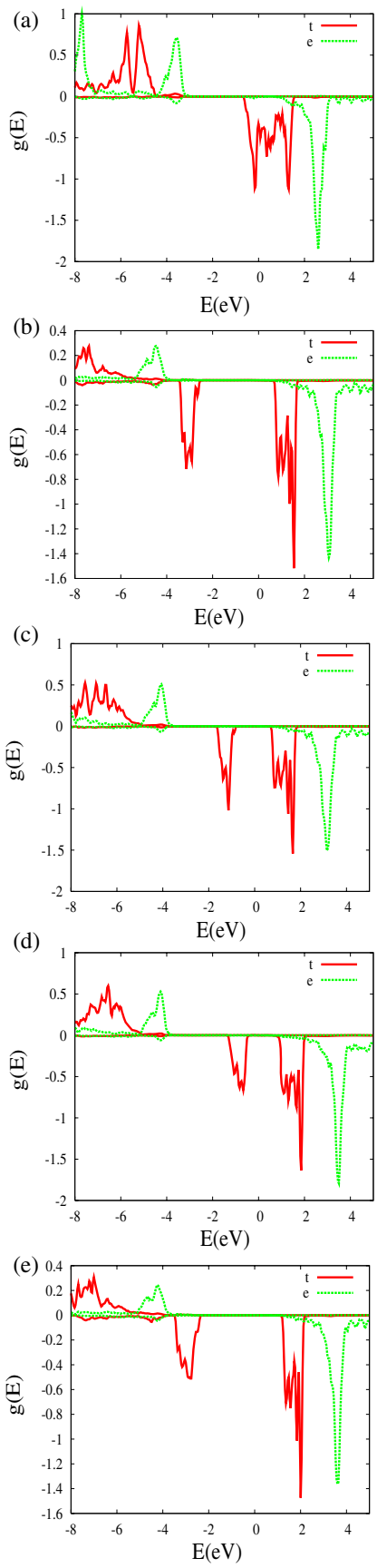

Figure 5. Projected DOS on d-Fe orbitals for the FeO. (a) $U = 0$ eV. (b)–(e) with $U = 4.3$ eV and using the calculation schemes $p(0)$-, $p(1/2)$-, $m2$ and $p'(1/2)$-LDA + U. The Fermi energy as zero has been chosen in this figure.

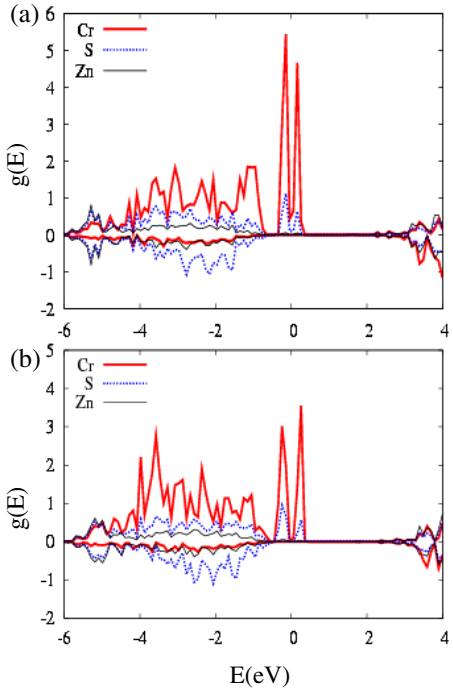

Figure 6. Projected DOS on Cr, S (those directly bonded to the Cr atom) and Zn atoms for the Cr-doped zinc chalogenides ($Cr_xZn_{1-x}S$, with $x = 1/32$) with $U = 3$ eV using (a) $p(1/2)$-LDA + U and (b) $p(0)$-LDA + U. The Fermi energy as zero has been chosen in this figure.

are the ones that mainly contribute to the IB. Comparing the results for $p(1/2)$-LDA + U and $p(0)$-LDA + U it is observed that the $p(0)$ scheme produces a larger IB splitting than the $p(1/2)$ scheme, according to the tendency observed in the Mott oxides. Whereas in [16], for $U > 6$ eV a metal insulator transition takes place with the $m2$-LDA + U scheme (similar to the $p(1/2)$-LDA + U), here it happens for $U > 3$ eV with the $p(0)$-LDA + U scheme.

3.5.2. Cr-doped chalcopyrite. The Cr-doped chalcopyrite $Cr_xGa_{1-x}CuS_2$ with $x = 1/16$ has an IB similar to the Cr-doped zinc chalogenides. The results of the chalcopyrite case show a similar behaviour with respect to the chalogenides case. It can be seen in figure 7, where the Projected DOS on d-Cr orbitals is shown using the $p(1/2)$-, $p(0)$- and $m2$-LDA + U schemes. From panels (a) and (c), the schemes $p(1/2)$ and $m2$ lead to similar results. However, the p(0)-LDA + U scheme leads to more accumulation of states inside the valence band (notice the scale change in the DOS for panel (b) with respect to panels (a) and (c)).

4. Conclusions

Both the occupation numbers as well as the effective Coulomb energy are crucial in the determination of the correlation effects from a computational point of view. However, there is some ambiguity in the definition of the occupation number matrix. There is no unique or rigorous way to define the occupation of localized atomic levels in a multi-atom system. Moreover,

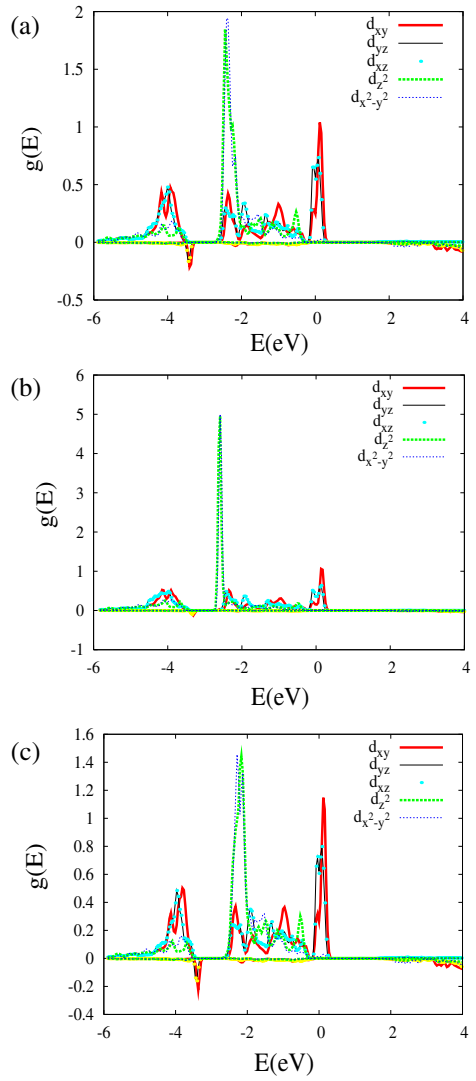

Figure 7. Projected DOS on d-Cr orbitals for the Cr-doped chalcopyrite $Cr_xGa_{1-x}CuS_2$ ($x = 1/16 = 0.0625$) with $U = 3$ eV using (a) $p(1/2)$-LDA $+ U$, (b) $p(0)$-LDA $+ U$ and (c) $m2$-LDA $+ U$. The Fermi energy as zero has been chosen in this figure.

it is usually straightforward to identify the atomic levels to be treated with the LDA/GGA $+ U$ approach in a given system.

In this work different definitions of the occupation number matrix consistent with the use of a non-orthogonal basis set are compared and discussed. Thus, we have used a general definition that conserves the total number of electrons, i.e. the trace of the occupation number matrix is equal to the total number of electrons. From this, we also have used a general definition that does not conserve the total number of electrons. This non-conserving choice includes some of the more used versions of the occupation number matrix. Therefore some of the representations used in this work, either have not been used or have been used only marginally in the literature. All of them, from the most novel to those most used ones, have been compared using different approaches and calculation implementations.

For typical transition-metal oxide bulk systems, the bandgap, magnetic moment and detailed electronic structures are investigated with respect to the choice of the occupation number matrix. This study has been carried out using both LDA$+U$ and GGA$+U$ methodologies. In general, with all the occupation schemes analysed, GGA $+ U$ leads to an increase in the gaps and magnetic moments with respect to LDA $+ U$.

In general the gaps decrease with the calculation scheme in the direction $p(\alpha) \geqslant p'(\alpha) > m2$-LDA/GGA $+ U$. For the magnetic moments there are differences until ± 1 μ_B between the different LDA/GGA $+ U$ calculation schemes when the same occupation matrices are used in order to obtain the magnetic moments. However, almost independently of the occupation matrices used in order to obtain the magnetic moments, the magnetic moments decrease with the calculation scheme used as $p(\alpha) \geqslant p'(\alpha) > m2$-LDA/GGA $+ U$. From the results, there is no definition that is clearly the best, and probably there is not a best definition, simply because of the ambiguity in the definition of the occupation.

Acknowledgments

This work has been supported by the GENESIS FW project of the National Spanish Programme CONSOLIDER (CSD2006-0004), by the European Commission through the funding of the project IBPOWER (ref. no. grant agreement 211640), and by La Comunidad de Madrid through the funding of the project NUMANCIA (Ref. No. S-0505/ENE/0310).

References

[1] Mott N F 1990 *Metal–Insulator Transition* (London: Taylor and Francis)
[2] Martin R M 2004 *Electronic Structure. Basis Theory and Practical Methods* (Cambridge: Cambridge University Press)
Ohno K, Esfarjani K and Kawazoe Y 1999 *Computational Materials Science. From ab initio to Monte Carlo Methods* (Berlin: Springer)
Parr R G and Yang W 1989 *Density Functional Theory of Atoms and Molecules* (New York: Oxford University Press)
Dobson J F, Vignale G and Das M P 1998 *Electron Density Functional Theory. Recent progress and New Directions* (New York: Plenum)
Flude P 1993 *Electron Correlations in Molecules and Solids* (*Springer Series in Solid-State Sciences*) 2nd edn (Berlin: Springer)
Szabo A and Ostlund N S 1996 *Modern Quantum Chemistry: Introduction to Advanced Electronic Structure Theory* (New York: Dover)
Anisimov V I (ed) 2000 *Strong Coulomb Correlations in Electronic Structure Calculations: Beyond the Local Density Approximation* (London: Gordon and Breach)
[3] Bredow T and Gerson A R 2000 *Phys. Rev.* B **61** 5194
Muscat J, Wander A and Harrison N M 2001 *Chem. Phys. Lett.* **342** 397
[4] Feng X-B and Harrison N M 2004 *Phys. Rev.* B **69** 035114
[5] Szotek Z and Temmerman W M 1993 *Phys. Rev.* B **47** 4029
[6] Pemmaraju C D, Archer T, Sánchez-Portal D and Sanvito S 2007 *Phys. Rev.* B **75** 045101
[7] Ren X, Leonov I, Keller G, Kollar M, Nekrasov I and Vollhardt D 2006 *Phys. Rev.* B **74** 195114
[8] Wang L, Maxisch T and Ceder G 2006 *Phys. Rev.* B **73** 195107
[9] Aryasetiawan F and Gunnarsson O 1995 *Phys. Rev. Lett.* **74** 3221

Faleev S V, van Schilfgaarde M and Kotani T 2004 *Phys. Rev. Lett.* **93** 126406
Li J L, Rignanese G M and Louie S G 2005 *Phys. Rev.* B **71** 193102
[10] Massidda S, Continenza A, Posternak M and Baldereschi A 1997 *Phys. Rev.* B **55** 13494
[11] Bengone O, Alouani M, Blochl P and Hugel J 2000 *Phys. Rev.* B **62** 16 392
[12] Shick A B, Liechtenstein A I and Pickett W E 1999 *Phys. Rev.* B **60** 10 763
[13] Cococcioni M and Gironcoli S 2005 *Phys. Rev.* B **71** 35105
[14] Han M J, Ozaki T and Yu J 2006 *Phys. Rev.* B **73** 045110
[15] Wierzbowska M, Sánchez-Portal D and Sanvito S 2004 *Phys. Rev.* B **70** 235209
[16] Tablero C 2005 *J. Chem. Phys.* **123** 114709
[17] Tablero C 2006 *Phys. Rev.* B **74** 195203
Tablero C 2007 *J. Chem. Phys.* **126** 164703
[18] Anisimov V I, Aryasetiawan F and Lichtenstein A I 1997 *J. Phys.: Condens. Matter* **9** 767
Lichtenstein A I, Anisimov V I and Zaanen J 1995 *Phys. Rev.* B **52** R5467
Dudarev S L, Botton G A, Savrasov S Y, Humphreys C J and Sutton A P 1998 *Phys. Rev.* B **57** 1505
[19] Dederichs R H, Bltigel S, Zeller R and Akai H 1984 *Phys. Rev. Lett.* **53** 2512
Solovyev I V, Dederichs R H and Anisimov V I 1994 *Phys. Rev.* B **50** 16861
[20] Pickett W E, Erwin S C and Ethridge E C 1998 *Phys. Rev.* B **58** 1201
[21] Eschrig H, Koepernik K and Chaplygin I 2003 *J. Solid State Chem.* **176** 482
[22] Hohenberg P and Kohn W 1964 *Phys. Rev.* B **136** 864
[23] Kohn W and Sham L J 1965 *Phys. Rev.* **140** A1133–8
[24] SIESTA code: Soler J M, Artacho E, Gale J D, García A, Junquera J, Ordejon P and Sánchez-Portal D 2002 *J. Phys.: Condens. Matter* **14** 2745 and references therein
[25] Ceperley D M and Alder B J 1980 *Phys. Rev. Lett.* **45** 566
[26] Perdew J P, Burke K and Ernzerhof M 1996 *Phys. Rev. Lett.* **77** 3865
Perdew J P, Burke K and Ernzerhof M 1997 *Phys. Rev. Lett.* **78** 1396
[27] Troullier N and Martins J L 1991 *Phys. Rev.* B **43** 1993
[28] Kleinman L and Bylander D M 1982 *Phys. Rev. Lett.* **48** 1425
Bylander D M and Kleinman L 1990 *Phys. Rev.* B **41** 907
[29] Sankey O F and Niklewski D J 1989 *Phys. Rev.* B **40** 3979
[30] Anisimov I, Zaanen J and Andersen O K 1991 *Phys. Rev.* B **44** 943
[31] Petukhov A G, Mazin I I, Chioncel L and Lichtenstein A I 2003 *Phys. Rev.* B **67** 153106
[32] Sawatzky G A and Allen J W 1984 *Phys. Rev. Lett.* **53** 2339
Hufner S *et al* 1984 *Solid State Commun.* **52** 793
[33] Iskenderov R N *et al* 1969 *Sov. Phys.—Solid State* **10** 2031
Messick L, Walker W C and Glosser R 1972 *Phys. Rev.* B **6** 3941
[34] Bowen H K *et al* 1975 *J. Solid State Chem.* **12** 355
[35] Powell R J and Spicer W E 1970 *Phys. Rev.* B **2** 2182
[36] Hufner S, Osterwaldr J, Riesterer T and Hullinger F 1984 *Solid State Commun.* **52** 793
Anisimov V I, Kuiper P and Nordgren J 1994 *Phys. Rev.* B **50** 8257